International Journal of Transportation Science and Technology xxx (xxxx) xxx

Contents lists available at ScienceDirect

International Journal of Transportation Science and Technology

journal homepage: www.elsevier.com/locate/ijtst

A theoretical model for evaluating the impact of connected and autonomous vehicles on the operational performance of turbo roundabouts

Marco Guerrieri

DICAM, University of Trento, via Mesiano 77, 38123 Trento, Italy

ARTICLE INFO

Article history:
Received 25 January 2023
Received in revised form 26 March 2023
Accepted 9 May 2023
Available online xxxx

Keywords:
Turbo roundabouts
Entry capacity
Total capacity
Automated vehicles
Central manager system

ABSTRACT

This article presents a methodology to estimate the entry capacity (EC) and the total capacity (TC) of basic turbo roundabouts under partial and fully connected and automated vehicles (CAVs) environments. Entry capacity calculations are partially based on capacity models and adjustment factors proposed by the HCM 7th edition, taking into account different proportions of CAVs in traffic streams. The proposed methodology was applied to a case study concerning a basic turbo roundabout with different traffic demand and market penetration levels (MPLs) of CAVs. It was assumed a traffic stream consisting of 100% passenger cars with MPLs of CAVs from 0% to 100%. The research proves that with the increase in MPLs of CAVs, entry capacities increase accordingly and delays and queues decrease. To maximize the total capacity, a control area was also hypothesized where CAVs start to communicate with a turbo roundabout manager system. The system should be able to distribute and channel CAVs, and therefore the entering flows between entry lanes and find the values of the maneuver distribution factors (α, β, γ, δ) between the right lane and the left lane of entries to maximize the TC for each origin–destination matrix of traffic flows.

1. Introduction

Well-designed turbo roundabouts can improve traffic operations compared to signalized or stopped-control road intersections when traffic demand is low to moderate (Mohebifard and Hajbabaie, 2021). Over the last fifteen years, turbo-roundabouts were mostly studied in terms of geometry, capacity (Fortuijn 2009; Tollazzi et al. 2011; Vasconcelos et al. 2014, Tollazzi, 2014; Corriere et al. 2013; Brilon, et al. 2014; Guerrieri et al., 2018), safety (Easa and You, 2023), life cycle, and environmental sustainability (Guerrieri, et al. 2015; Mauro and Guerrieri, 2016). Entry capacity is one of the most important measures of effectiveness (MOE) and has been widely used as a useful indicator of performance. According to Yap, et al. (2013), entry capacity (EC) is the maximum inflow from a roundabout entry with saturated demand, where at least one vehicle is always queued at the yield line of the entry lane ready to enter any available acceptable gap in the circulating flow. Gap acceptance theory is commonly used for modelling the relationships between turbo roundabout entry capacity, circulating flow, critical gap, follow-up time and distribution of gaps in circulating flow. Some of the most used models for entry

Peer review under responsibility of Tongji University and Tongji University Press.
E-mail address: marco.guerrieri@unitn.it

https://doi.org/10.1016/j.ijtst.2023.05.001
2046-0430/

capacity estimation at turbo roundabouts are based on the outcomes of Akcelik (1994), Rodegerdts et al. (2007), Brilon et al. (1997), Troutbeck (1989) and Wu (2001). A proper critical gap is required to predict entry capacity with the gap acceptance model. A common strategy is to assume values from the literature, such as those suggested by the Highway Capacity Manual (HCM) or values estimated by calibration of a critical gap at each location (Song et al., 2022).

For roundabouts, two additional definitions of capacity can be given (Mauro, 2010):

- Simple Capacity (SC): is the first capacity value that is recorded at an entry for a uniform increase in the flows that make up the traffic demand;
- Total Capacity (TC): with respect to a given percentage distribution of entering traffic, TC is the sum of the entering flows from the entries under the condition that for each entry the entering flow is equal to its capacity.

The current changes in vehicle performance because of the innovation of the modern automotive industry, entails that the turbo roundabouts need to be examined in a wider range of aspects. In particular, the future introduction of Connected and Autonomous Vehicles (CAVs) may remarkably impact safety and traffic performance. Thanks to the advancement of communication technologies between vehicles and infrastructure (i.e. V2V and V2I systems) CAVs provide new opportunities for traffic control. Bilateral communication can increase the quantity of information that can be inferred and offers greater cooperation capability between vehicles and roads. Also, V2V and V2I technologies ensure much less perception-reaction time than human-driven vehicles (HDVs). In addition, CAVs will be equipped with cooperative adaptive cruise control (CACC) systems that permit vehicles in a platoon to maintain smaller space and time headways, as compared to adaptive cruise control (ACC), with improvement in safety as well as fuel efficiency (Jiang, et al. 2022).

Although CAVs have been tested on public roads, Autonomous Guidance, Navigation and Control systems are still in the early stages. It is estimated that there will be a long-term period in order CAVs will coexist with traditional vehicles on public roads (Zmud et al., 2018). CAVs will be controlled by sensors and computers; therefore, CAVs will have quicker reaction times than human drivers. Consequently, shorter gaps can be accepted during maneuvers at road intersections.

For future application to mobility systems, road operators need to understand how road performances, in terms of capacities, delays and level of services, would be affected by the increasing penetration level of CAVs (Guerrieri, 2021). Understanding the effects of CAVs on road networks is crucial for future transportation control, policymaking, and road and highway design (Jiang, et al., 2022).

A few researchers have analysed the application of CAVs on traditional roundabouts (Jiang, et al. 2022, Zhao et al., 2018; Martin-Gasulla and Elefteriadou, 2019). Some research demonstrates that roundabouts are more efficient than signalized intersections for a fleet of 100% CAVs and mixed traffic conditions (Gill et al., 2015; Wu and Zhu, 2021). Nevertheless, during the first introduction period of CAVs the capacity of the road systems could decrease due to the larger headways between CAVs and traditional vehicles that for safety reasons are required (Martin-Gasulla et al., 2019). However, the increment in market penetration levels of CAVs will improve traffic operations in terms of capacity, delay, queue and emissions (Anagnostopoulos and Kehagia, 2020; Mohebifard and Hajbabaie, 2021).

The current HCM procedures (HCM 7th Edition, 2022) for roundabout performance analysis are established for both human-driven vehicles (HDVs) and CAVs. In particular, the HCM allows for establishing the CAV-adjusted capacity values for different roundabout layouts (one or two entry lanes, and one or two circulating lanes) and various proportions of CAVs in the traffic stream. However, CAV-adjusted capacity values have been obtained by microsimulations and therefore they can only approximate the potential effects of CAVs on roundabout capacities. Moreover, the HCM procedure can be applied only to conventional roundabouts (HCM 7th Edition, 2022 , AASHTO, 2011).

To address these limitations, this paper introduces a methodology based on closed-form models to calculate the entry capacity (EC) and the total capacity (TC) of turbo roundabouts with a partial or fully automated fleet of vehicles. The theoretical model was applied to a case study concerning a basic turbo roundabout with different traffic demand levels and market penetration levels (MPLs) of CAVs. It was assumed a traffic stream consisting of 100% passenger cars; the percentage of CAVs in the traffic stream varies from 0% to 100%, with a continuous increment in MPLs.

It is useful to underline that various modeling assumptions used in this research are consistent with the current knowledge in traffic engineering, even if at the moment there is a lack of experimental data that would make them reliable (Tumminello, et al. 2022). As a matter of fact, rules and technology systems on CAVs are still in progress and no empirical data from real-word are available for calibrating both microscopic traffic simulations and closed-form capacity models. Nevertheless, the outcomes of this study point out the potential benefits related to the introduction of different MPLs of CAVs in traffic streams for turbo roundabouts. As a matter of fact, though the outcomes are affected by the assumptions regarding the critical gap $t_{c,CAVs}$ and follow-up time $t_{f,CAVs}$ of CAVs, the results revealed that CAVs can improve turbo roundabouts performances in terms of increasing EC and TC and reducing queues and delays.

The remainder of this paper is organized as follows: section "Entry capacity models: general considerations" provides a detailed description of the methodology for entry capacity, delay and queue estimation at turbo roundabout entries, taking into consideration the effect of several MPLs of CAVs. Section "CAVs coordination to maximize the total capacity" presents a closed-form model for the TC estimation and a procedure for maximizing the total capacity profit the potential offered by CACC and CAVs technologies and by a central manager system to optimize vehicle trajectories in the shared lanes at entries. Finally, the section "Conclusions" concludes this article and proposes future research directions.

2. Entry capacity models: General considerations

In turbo roundabouts, entry lanes, circulating and exit lanes are physically divided by unsurmountable curbs. Users approaching turbo roundabouts must select the lane along the entry arm to make their desired manoeuvres (through, left-turn or right-turn manouvres). All vehicles coming from all arms must give priority to circulating vehicles. In basic turbo roundabouts, through-manoeuvres and left-turn manoeuvres come into conflict with the traffic streams in the outer and inner circulating lanes (arms 1 and 3 of Fig. 2). Therefore, according to the gap-acceptance model, these vehicles have to wait for the simultaneous presence of gaps wide enough (i.e. greater than the user's critical gap) between vehicles belonging to traffic streams of the circulating inner and outer lanes. Instead, the right-turn manoeuvres occur in the same manner as at conventional roundabouts. The previous considerations make clear why the estimation of the entry capacity (EC) and total capacity (TC) at turbo-roundabouts necessitates a prior evaluation of the capacities at each entering lane, which in general change from one another. Therefore, for the generic arm j, (j = 1,2,3, 4), the capacity of the right lane $C_{j,R}$ and left lane $C_{j,L}$ must be calculated separately through a lane-by-lane analysis (Akcelik, 1997).

The overall procedure applied in this research for the calculation of the measures of effectiveness (MOE) of turbo roundabouts is summarized in the flowchart of Fig. 1.

Fig. 2 illustrates the traffic streams at entry lanes for three particular traffic distribution matrices: $P_{O/D}$ 1 = 100% of entering vehicles turn right, $P_{O/D}$ 2: 100% of entering vehicles cross the roundabout, $P_{O/D}$ 3 = 100% of entering vehicles turn left. According to Fig. 2, denoting with α, β, γ, δ the maneuver distribution factors between the right lane and the left lane, of entries 1, 2, 3, and 4 respectively, the entering, circulating and exit volumes can be calculated as follows:

- *entering volumes:*

$$v_{e1,R} = \alpha \cdot v_{1,2} \tag{1}$$

$$v_{e1,L} = (1-\alpha) \cdot v_{1,2} + v_{1,3} + v_{1,4} \tag{2}$$

$$v_{e1} = v_{1,R} + v_{1,L} \tag{3}$$

$$v_{e2,R} = v_{2,3} + (1-\beta) \cdot v_{2,4} \tag{4}$$

$$v_{e2,L} = \beta \cdot v_{2,4} + v_{2,1} \tag{5}$$

$$v_{e2} = v_{2,R} + v_{2,L} \tag{6}$$

$$v_{e3,R} = \gamma \cdot v_{3,4} \tag{7}$$

$$v_{e3,L} = (1-\gamma) \cdot v_{3,4} + v_{3,1} + v_{3.2} \tag{8}$$

$$v_{e3} = v_{3,R} + v_{3,L} \tag{9}$$

$$v_{e4,R} = v_{4,1} + (1-\delta) \cdot v_{4,2} \tag{10}$$

$$v_{e4,L} = \delta \cdot v_{4,2} + v_{4,3} \tag{11}$$

$$v_{e4} = v_{4,R} + v_{4,L} \tag{12}$$

- *circulating volumes:*

$$v_{c,1e} = (1-\delta) \cdot v_{4,2} + v_{3,2} \tag{13}$$

$$v_{c,1i} = \delta \cdot v_{4,2} + v_{4,3} \tag{14}$$

$$v_{c,1} = v_{c,1e} + v_{c,1i} \tag{15}$$

$$v_{c,2} = v_{4,3} + v_{1,3} + v_{1,4} \tag{16}$$

$$v_{c,3i} = \beta \cdot v_{2,4} + v_{2,1} \tag{17}$$

$$v_{c,3e} = (1-\beta) \cdot v_{2,4} + v_{1,4} \tag{18}$$

$$v_{c,3} = v_{c,3e} + v_{c,3i} \tag{19}$$

$$v_{c,4} = v_{2,1} + v_{3,1} + v_{3,2} \tag{20}$$

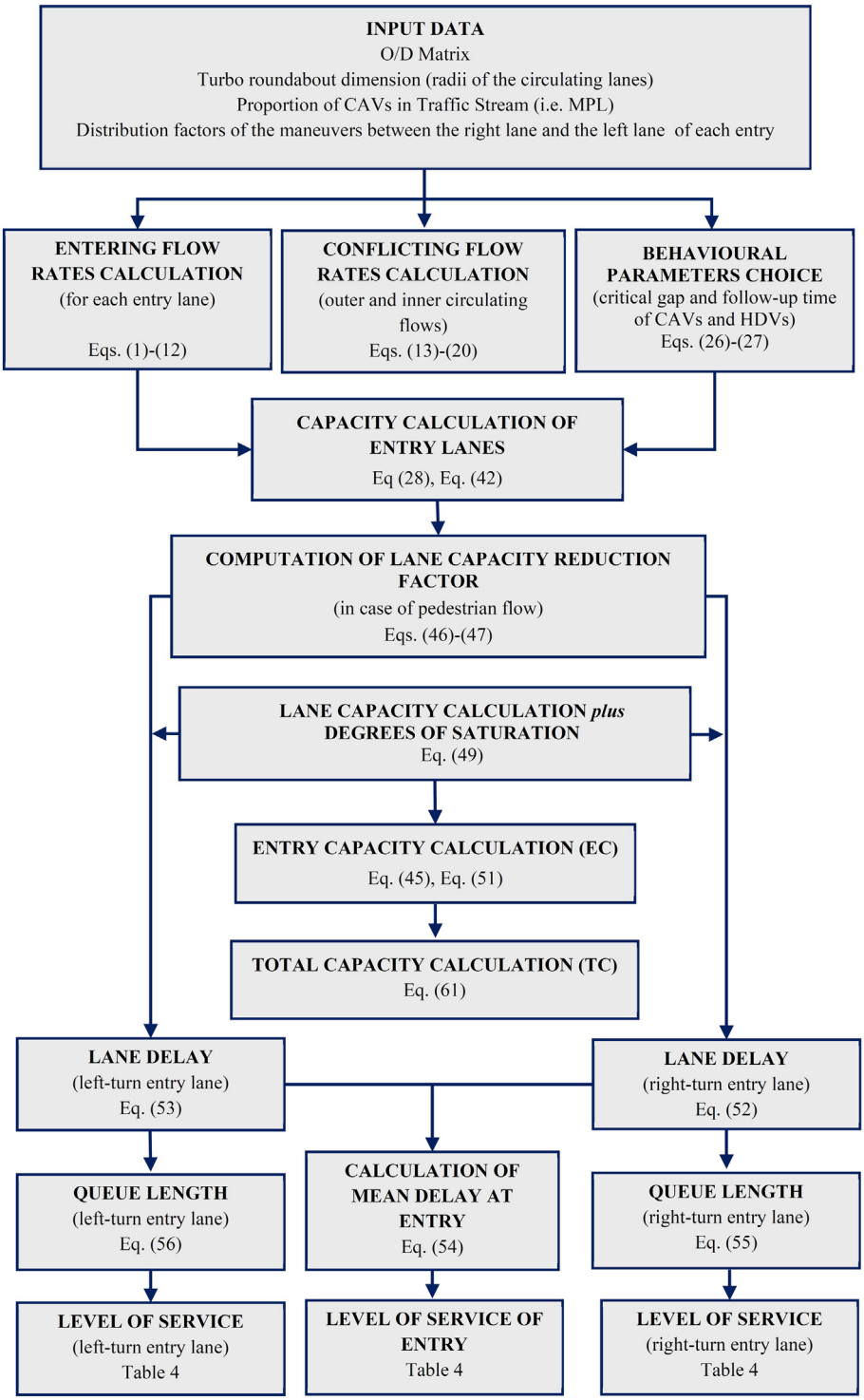

Fig. 1. Procedure for the MOE estimation at turbo roundabouts in CAVs environment.

- *exit volumes:*

$$v_{u,1} = v_{3,1} + v_{2,1} + v_{4,1} \tag{21}$$

$$v_{u,2} = v_{3,2} + v_{4,2} + v_{1,2} \tag{22}$$

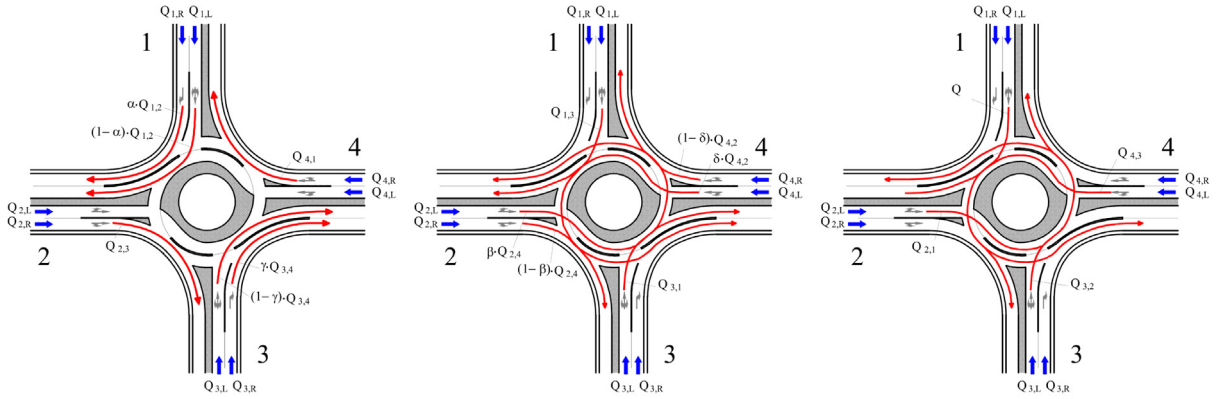

Fig. 2. Traffic streams at entries for different origin–destination traffic matrices. a) $P_{O/D}$ 1 = 100% of entering vehicles turn right; b) $P_{O/D}$ 2: 100% of entering vehicles cross the turbo roundabout; c) $P_{O/D}$ 3 = 100% of entering vehicles turn left.

$$v_{u,3} = v_{4,3} + v_{1,2} + v_{2,3} \tag{23}$$

$$v_{u,4} = v_{1,4} + v_{2,4} + v_{3,4} \tag{24}$$

2.1. Capacity model for the right lane (arms 1 and 3)

Given the geometric and traffic regulation analogies with conventional roundabouts, the capacity at the right-turn lane ($C_{j,R}$) can be estimated by fitting the model of the HCM 7th Edition, 2022. According to the HCM model, in steady-state traffic conditions, the entry capacity of the right-turn lane for the j-th arm (cf. Fig. 2), can be calculated using the following equation in function of the MPLs of automated vehicles:

$$C_{j,R} = f_A \cdot A \cdot e^{-f_B \cdot B \cdot v_{c,i}} \tag{25}$$

$C_{j,R}$ = entry lane capacity, adjusted for CAVs and heavy vehicles (pc/h);
A = intercept parameter;
B = slope parameter;
$v_{c,j}$ = conflicting flow rate (pc/h);
f_A = adjustment factor for the intercept parameter.
f_B = adjustment factor for the intercept parameter.

The HCM gives the Capacity Adjustment Factors for CAVs shown in Table 1. The values of f_A and f_B in Table 1 have been deduced by traffic microsimulations.

The right-turn lanes of turbo roundabouts can be assimilated to a conventional roundabout with one-lane entry conflicted by one circulating lane (Guerrieri et al., 2015); therefore, it results: A = 1,380, B = 1.02×10^{-3}, follow up-time = 2.61 s, critical

Table 1
Capacity adjustment factors by penetration rate of CAVs for conventional roundabouts (HCM 7th Edition, 2022).

Proportion of CAVs in Traffic Stream	1-Lane Entry				2-Lane Entry					
	1 Circulating Lane		2 Circulating Lanes		1 Circulating Lane, Both Lanes		2 Circulating Lanes, Left Lane		2 Circulating Lanes, Right Lane	
Traffic Stream	f_A	f_B	f_A	f_B	f_A	f_B	f_A	f_B	f_A	f_B
0	1	1	1	1	1	1	1	1	1	1
20	1.1	1	1	1	1.05	1	1	0.99	1.05	0.96
40	1.1	1	1.1	1	1.12	1	1.1	0.96	1.12	0.93
60	1.2	0.9	1.2	0.9	1.22	0.9	1.2	0.92	1.2	0.87
80	1.3	0.9	1.3	0.9	1.29	0.9	1.3	0.89	1.27	0.84
100	1.4	0.9	1.4	0.9	1.35	0.9	1.4	0.85	1.34	0.8

gap = 4.98 s. In this research the effect of different proportions of CAVs on entry capacity is estimated by using proper mean values of critical gap and follow-up time, as follows:

$$t_{c,m} = \frac{t_{c,CAVs} \cdot MPL + t_{c,H} \cdot (1 - MPL)}{100} \tag{26}$$

$$t_{f,m} = \frac{t_{f,CAVs} \cdot MPL + t_{f,H} \cdot (1 - MPL)}{100} \tag{27}$$

In which $t_{c,H}$ and $t_{f,H}$ are the critical gap and follow-up time of traditional vehicles, $t_{c,CAVs}$ and $t_{f,\ CAVs}$ are the critical gap and the follow-up time of CAVs, MPL is the market penetration level of CAVs; finally, $t_{c,m}$ and $t_{f,m}$ are the mean values associated to mixed traffic of traditional vehicles and CAVs.

Therefore, the entry capacity model can be expressed by Eq. (28):

$$C_{j,R} = A_m \cdot e^{-B_m \cdot v_{c,i}} \tag{28}$$

In which

$$A_m = 3600/t_{f,m} \tag{29}$$

$$B_m = [t_{c,m} - (t_{f,m}/2)]/2 \tag{30}$$

As it is well known, operating a cooperative adaptive cruise control system may reduce the reaction times of the vehicle guide systems, consequently $t_{c,CAVs}$ e $t_{f,\ CAVs}$ can be estimated as:

$$t_{c,CAVs} = \eta \cdot t_{c,H} \tag{31}$$

$$t_{f,CAVs} = \Psi \cdot t_{c,H} \tag{32}$$

The values of the reduction coefficients η and Ψ were obtained through a calibration procedure imposing that the maximum deviations between the HCM capacity model and the proposed one be less than 5% for each conflicting flow rate. In light of these considerations, and assuming the calibrated values η = 0.85 and Ψ = 0.73, it results: $t_{c,CAVs}$ = 4.2 s and $t_{f,\ CAVs}$ = 1.9 s. Table 2 shows the values of $t_{c,m}$, $t_{f,m,}$ A_m and B_m for different MPLs, instead, Fig. 3a) and b) show the comparisons between the HCM entry capacity model and the proposed entry capacity model for two very different market penetration rates of CAVs (e.g. MPL = 20% and MPL = 100%). As shown in Fig. 4, the deviations between the two capacity models are always less than 4% even for conflicting flow rates close to 1600 pc/h.

2.2. Capacity model for the left lane (arms 1 and 3)

Considering the left lanes' operational conditions, the left lane capacity can be estimated as described in this section. For the sake of simplicity, we first analyse the arm n. 1 of Fig. 2. Consider entering vehicles belonging to the flow $v_{1,L}$ whose motion is hindered by the conflict flow rate on outer and inner circulating lanes ($v_{c,1e}$ and $v_{c,1i}$ respectively) in front the arm 1. The flows are in stationary conditions. Furthermore, be: $t_{c,m}$ and $t_{f,m}$ the mean psycho technical parameters (cf. Eq. (26) and Eq. (27) associated to vehicles (HDVs and CAVs) in the entry lane with a flow $v_{1,L}$, $f(\tau)$ the probability density function of vehicle headways of the circulation flow, $n(\tau)$ the number of vehicles of the left lane of the arm 1 which performs the desired maneuver, entering the time gap of value τ and $\bar{n}$ the average number of the vehicles on the left lane of arm 1 which enter the gaps in the circulating flow, completing the desired maneuver. Given these conditions, it follows (Yap, et al. 2013; Brilon et al. 1993; Brilon et al, 1997):

$$\bar{n} = \int_0^\infty n(\tau) \cdot f(\tau) \cdot d\tau \tag{33}$$

The capacity of the left lane of arm 1 is given by the ratio between $\bar{n}$ and the average headway in the circulating flow $\bar{\tau} = 1/v_{c,j}$:

Table 2
Estimated values of critical gag, follow-up time and coefficients A_m and B_m.

MPL [%]	$t_{f,m}$ [s]	$t_{c,m}$ [s]	A_m	B_m
0	2.61	4.98	1380	0.001020
20	2.47	4.82	1459	0.000997
40	2.33	4.67	1548	0.000973
60	2.18	4.51	1649	0.000950
80	2.04	4.36	1763	0.000926
100	1.90	4.20	1895	0.000903

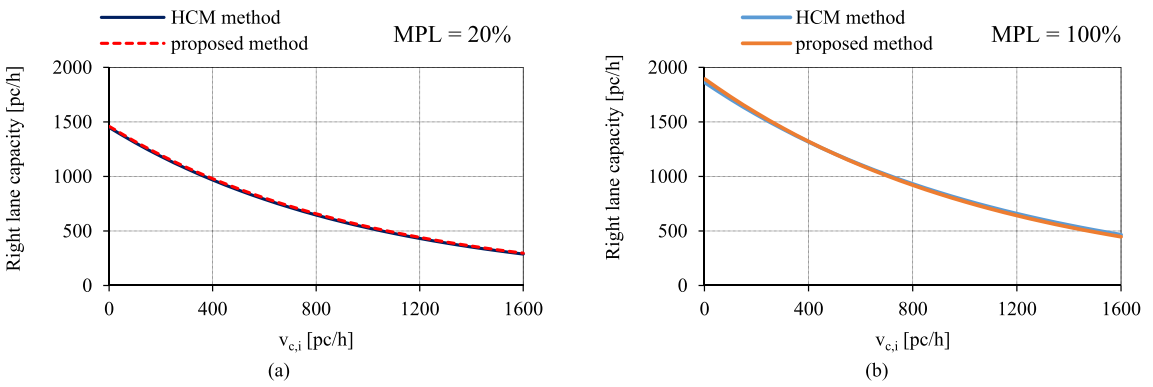

Fig. 3. Comparisons between capacity curves (HCM model vs proposed model) for two market penetration levels. a) MPL = 20%; b) MPL = 100%.

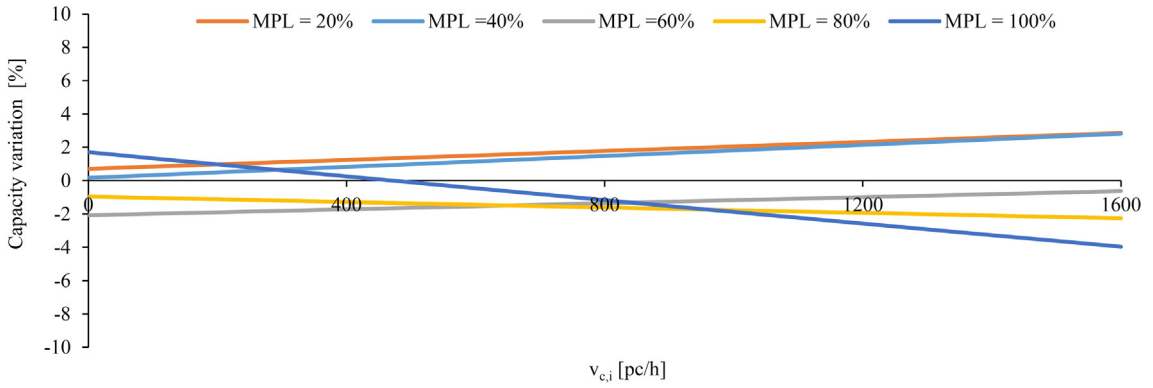

Fig. 4. Capacity percentage variation (proposed model vs HCM model).

$$c = \frac{\bar{n}}{\bar{\tau}} = v_{c,j} \cdot \int_0^{\infty} n(\tau) \cdot f(\tau) \cdot d\tau \tag{34}$$

Assume the behavioral model described in Fig. 5 (Mauro, 2010), it results that 0 vehicles overpass the yield line in the presence of a gap $\tau < t_{c,m}$, 1 vehicle overpass the yield line if $t_{c,m} \leq \tau < t_{c,m} + t_{f,m}$, 2 vehicles overpass the yield line if $t_{c,m} + t_{f,m} \leq \tau < t_{c,m} + 2\ t_{f,m}$, etc.

The step law $n = n(\tau)$ exemplified in Fig. 5 can be approximated with a continuous function represented by a straight line with an intercept t_0, slope coefficient $1/t_{f,m}$; then, it follows:

$$T_c = T_0 + 0.5 \cdot t_{f,m} \tag{35}$$

$$n(\tau) = \frac{\tau - T_0}{T_f} \tag{36}$$

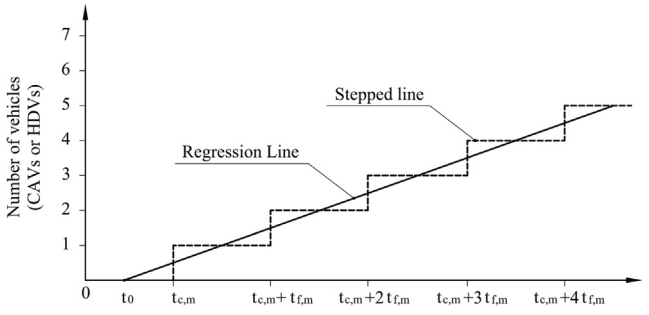

Fig. 5. Number of vehicles that overpass the yield line in function of the τ value.

Considering an exponential law for the headways τ process

$$f(\tau) = v_{c,j} \cdot e^{-v_{c,j} \cdot \tau} \tag{37}$$

by previous relationships, it yields:

$$C_{j,L} = v_{c,j} \cdot \int_0^{\infty} \frac{\tau - T_0}{t_{f,m}} \cdot v_{c,j} \cdot e^{-v_{c,j} \cdot \tau} \cdot d\tau = \frac{1}{t_{f,m}} \cdot e^{-v_{c,j} \cdot \tau} \tag{38}$$

by considering the step law in Fig. 5, after some passages the following equation is obtained (Mauro, 2010):

$$C_{j,L} = v_{c,j} \cdot \frac{e^{-v_{c,j} \cdot \frac{t_{c,m}}{3600}}}{1 - e^{-v_{c,j} \cdot \frac{t_{f,m}}{3600}}} \tag{39}$$

Eq. (39) can be adopted for estimating the capacity of the left lanes of arms 1 and 3.

It can be noted that the circulating flow in front of the arm j (with j = 1 or 3) $v_{c,j}$ is the sum of the inner and outer circulating flows ($v_{c,ji}$ and $v_{c,je}$, respectively). Therefore the traffic stream $v_{1,L}$ must yield not only to the traffic stream of the outer lane of the ring $v_{c,je}$, but also to the traffic stream of the inner lane of the ring $v_{c,ji}$.

Thus, not all gaps of acceptable length in the outer lane will normally be available for use by users of the traffic stream $v_{1,L}$. This is because these users must cross the flow $v_{c,je}$, overcome the outer lane and enter the inner lane whose flow is $v_{c,ji}$. The magnitude of the correlated impedance depends on the degree of saturation (flow/capacity) of the inner circulating lane and can be expressed by the following equation:

$$k = 1 - \frac{v_{c,ji}}{C_i} \tag{40}$$

The capacity C_i of the inner circulating lane depends on its radius R_i. Fig. 6 summarises the typical values of the inner and outer circulating lanes radii in front of each arm of a basic turbo roundabout.

In this research it was assumed $C_{i,max}$ = 2000 pc/h for a radius R_{max} = 25 m, $C_{i,min}$ = 1600 pc/h for a radius R_{min} = 7.5 m (Mauro, 2010) and a linear relationship between capacity and radius, as follows:

$$C_i = C_{i,max} - \frac{C_{i,max} - C_{i,min}}{R_{max} - R_{min}} \cdot (R_{max} - R_i) = 2000 - 22.857 \cdot (25 - R_i) \tag{41}$$

Finally, we obtain the following relationship:

$$C_{j,L} = (1 - \frac{v_{c,ji}}{C_i}) v_{c,j} \cdot \frac{e^{-v_{c,j} \cdot \frac{t_{c,m}}{3600}}}{1 - e^{-v_{c,j} \cdot \frac{t_{f,m}}{3600}}} \tag{42}$$

Eq. (42) can be used for estimating the capacity of the left lanes of arms 1 and 3.

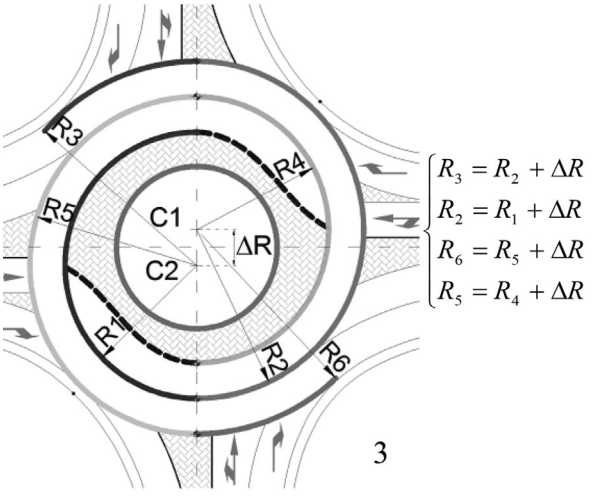

ΔR = 4.20 m (Lane width = 3.50 m)				
Radius	Mini	Standard	Medium	Larg
R_1 [m]	10.50	12.00	15.00	20.0
R_2 [m]	14.70	16.20	19.20	24.2
R_3 [m]	18.90	20.40	23.40	28.4
R_4 [m]	10.50	12.00	15.00	20.0
R_5 [m]	14.70	16.20	19.20	24.2
R_6 [m]	18.90	20.40	23.40	28.4
ΔR = 4.45 m (Lane width = 3.75 m)				
R_1 [m]	10.50	12.00	15.00	20.0
R_2 [m]	14.95	16.45	19.45	24.4
R_3 [m]	19.40	20.90	23.90	28.9
R_4 [m]	10.50	12.00	15.00	20.0
R_5 [m]	14.95	16.45	19.45	24.4
R_6 [m]	19.40	20.90	23.90	28.9
ΔR = 4.70 m (Lane width = 4.00 m)				
R_1 [m]	10.50	12.00	15.00	20.0
R_2 [m]	15.20	16.70	19.70	24.7
R_3 [m]	19.90	21.40	24.40	29.4
R_4 [m]	10.50	12.00	15.00	20.0
R_5 [m]	15.20	16.70	19.70	24.7
R_6 [m]	19.90	21.40	24.40	29.4

Fig. 6. Typical radii values (data from Tollazzi, 2014).

2.3. Entry capacity (EC)

The entry capacity can be estimated taking into consideration, entering volumes, the capacity of the right and left lanes and their degrees of saturation, as follows:

$$x_{eJ,R} = \frac{v_{eJ,R}}{C_{J,R}} \tag{43}$$

$$x_{eJ,L} = \frac{v_{eJ,L}}{C_{J,L}} \tag{44}$$

$$C_J = \frac{v_{eJ,R} + v_{eJ,L}}{\max\left[\frac{v_{eJ,R}}{C_{J,R}}; \frac{v_{eJ,L}}{C_{J,L}}\right]} \tag{45}$$

with:

C_j = capacity of the entry j;
$xe_{j,R}$ = degree of saturation of the right lane at entry j;
$xe_{j,L}$ = degree of saturation of the left lane at entry j;
$ve_{j,R}$ = flow rate of the right lane at the entry j;
$ve_{j,L}$ = flow rate of the left lane at the entry j.

Pedestrian flows can reduce turbo roundabout capacity if they assert the right-of-way. Above all in case of low values of entering vehicular flows, pedestrians can effectively function as extra conflicting vehicles and thus decrease the vehicular capacity of the entry at turbo-roundabouts.

The model of Eqs. (46)–(51), is based on the German method (Mauro, 2010) and can be used to assess this effect. The capacity reduction factors are given below.

Arms 1 and 3 (two circulating lanes in front of each entry):

$$M_{j,R} = (1119,5 - 0,715 \cdot v_{c,je} - 0,644 \cdot v_j^{ped} + 0,00073 \cdot v_{c,je} \cdot v_j^{ped})/(1069 - 0,65 \cdot v_{c,je}) \tag{46}$$

$$M_{j,L} = [1119,5 - 0,715 \cdot (v_{c,je} + v_{c,ji}) - 0,644 \cdot v_j^{ped} + 0,00073 \cdot (v_{c,je} + v_{c,ji}) \cdot v_j^{ped}]/[1069 - 0,65 \cdot (v_{c,je} + v_{c,ji})] \tag{47}$$

Arms 2 and 4 (one circulating lanes in front of each entry):

$$M_{j,R} = M_{j,L} = (1119,5 - 0,715 \cdot v_{c,j} - 0,644 \cdot v_j{}^{ped} + 0,00073 \cdot v_{c,j} \cdot v_j{}^{ped})/(1069 - 0,65 \cdot v_{c,j}) \tag{48}$$

$$C_{J,R}^{ped} = C_{j,R} \cdot M_{j,R} \tag{49}$$

$$C_{J,L}^{ped} = C_{j,L} \cdot M_{j,L} \tag{50}$$

$$C_j^{ped} = \frac{v_{eJ,R} + v_{eJ,L}}{\max\left[\frac{v_{eJ,R}}{C_{J,R}^{ped}}; \frac{v_{eJ,L}}{C_{J,L}^{ped}}\right]} \tag{51}$$

where:

$M_{j,R}$ = right lane pedestrian capacity reduction factor of the entry j;
$M_{j,L}$ = left lane pedestrian capacity reduction factor of the entry j;
$C_{j,R}{}^{ped}$ = right lane capacity of the entry j considering impact of pedestrians [pc/h];
$C_{j,L}{}^{ped}$ = left lane capacity of the entry j considering the impact of pedestrians [pc /h];
$C_{j,R}$ = right lane capacity of the entry j (no pedestrians crossing, only vehicles) [pc /h];
$C_{j,\,L}$ = left lane capacity of the entry j (no pedestrians crossing, only vehicles) [pc/h];
$v_j{}^{ped}$ = pedestrian flow at the entry j [p/h].

Eq. (51) shows that the capacity of the generic entry j varies with the capacity of the right and left lanes, and thus with: circulating flows at the circulatory carriageway; users behavior (through parameters $t_{c,m}$, $t_{f,m}$); traffic demand balance at entry arms; degrees of saturation; distribution factors of the maneuvers between the right lane and the left lane (through the distribution factors α, β, γ, δ); turbo-roundabout dimension (through the radius R_i) proportion of CAVs in traffic stream (through MPLs); pedestrian flows.

The maximum entry capacity value is reached when the degree of saturation of the right lane $x_{j,R}$ is equal to the degree of saturation of left lane $x_{ej,L}$. Only in this particular circumstance, it results: $C_j{}^{ped} = C_{j,R}{}^{ped} + C_{j,L}{}^{ped}$, instead if $x_{ej,R} \neq x_{ej,L}$ the entry capacity assumes a lower value than the sum of the single lane capacities (i.e. $C_j{}^{ped} < C_{j,R}{}^{ped} + C_{j,L}{}^{ped}$).

Figs. 7–9, exemplifies the capacity variations of entry 1 (cf. Fig. 2) in function of the degree of saturation of entry lanes, MPLs and circulating flows. As summarized in Table 3, in Scenario 1 the circulating flows in the outer and inner lanes are balanced ($v_{c,1e}$ = 500 pc/h, $v_{c,1i}$ = 500 pc/h), instead, in the other two scenarios the circulating flows in front of the arm 1 are unbalanced (for Scenario 2: $v_{c,1e}$ = 750 pc/h, $v_{c,1i}$ = 250 pc/h, for Scenario 3: $v_{c,1e}$ = 250 pc/h, $v_{c,1i}$ = 750 pc/h).

A fully automated vehicle's environment (MPL = 100%) generates significant increases in entry capacity compared to a fully human-driven environment (MPL = 0%). For example, in the case of Scenario 1, the capacity increase reaches 57%. These outcomes are consistent with the general results obtained from several types of research on the effects of CAVs on road intersections and highways.

Given the symmetry of the basic turbo roundabout layout in Fig. 2, the same results (cf. Figs. 7–9) can be obtained for the entry 3.

2.4. Delay and queue estimation

In traffic engineering, delay and queue lengths play a key role among the measures of effectiveness MOE of road intersections. Queues result from the waiting phenomena that users may suffer at the entries. Instead, delays are the result of queuing up (Mauro, 2010). After determining the capacity and the degree of saturation of each entry lane, the control delay of the right and left lanes at the generic entry J can be estimated from the following equations (HCM 7th Edition, 2022):

$$D_{J,R}^{ped} = \frac{3600}{C_{J,R}^{ped}} + 900 \cdot T \cdot \left[\frac{v_{eJ,R}}{C_{J,R}^{ped}} - 1 + \sqrt{\left(\frac{v_{eJ,R}}{C_{J,R}^{ped}} - 1 \right)^2 + \frac{\left(\frac{3600}{C_{J,R}^{ped}} \right) \cdot \left(\frac{v_{eJ,R}}{C_{J,R}^{ped}} \right)}{450 \cdot T}} \right] + 5 \cdot \min \left[\frac{v_{eJ,R}}{C_{J,R}^{ped}}, 1 \right] \quad (52)$$

$$D_{J,L}^{ped} = \frac{3600}{C_{J,L}^{ped}} + 900 \cdot T \cdot \left[\frac{v_{eJ,L}}{C_{J,L}^{ped}} - 1 + \sqrt{\left(\frac{v_{eJ,L}}{C_{J,L}^{ped}} - 1 \right)^2 + \frac{\left(\frac{3600}{C_{J,L}^{ped}} \right) \cdot \left(\frac{v_{eJ,L}}{C_{J,L}^{ped}} \right)}{450 \cdot T}} \right] + 5 \cdot \min \left[\frac{v_{eJ,L}}{C_{J,L}^{ped}}, 1 \right] \quad (53)$$

where, for the entry j, $D_{j,R}{}^{ped}$ is the average control delay at the right lane, $D_{j,L}{}^{ped}$ is the average control delay at the left lane and T is the analysis period (h) (T = 0.25 h for a 15-min analysis). The other variables in Eqs. (52) and (53) are defined in the previous section of this article. As can be immediately observed from Eqs. (52) and (53), the average control delay for a given lane is a function of the lane's capacity and degree of saturation.

To estimate the level of service (LOS) at each entry lane, the threshold limits summarized in Table 4 and established by HCM 7th Edition, 2022 can be adopted.

Therefore, it is possible to assign the LOS for each entry lane. However, if a global information is needed, it may still be helpful to establish the average delay of the entry j by attributing different weights to the delays of the right and left lanes of each entrance according to the respective traffic demand, as follows:

$$D_j = \frac{D_{J,R}^{ped} \cdot v_{J,R} + D_{J,L}^{ped} \cdot v_{J,L}}{v_{J,R} + v_{J,L}} \quad (54)$$

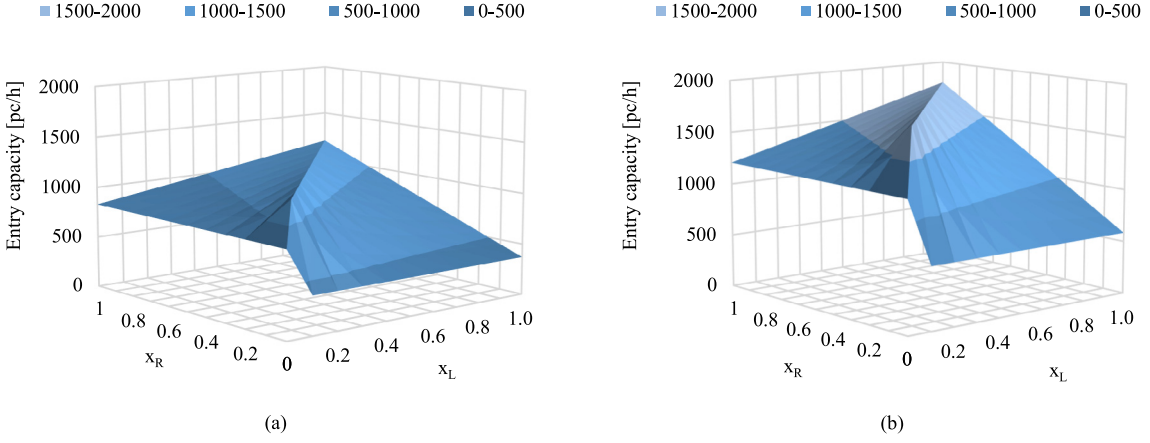

Fig. 7. Entry capacity, Scenario 1. a) MPL = 0%; b) MPL = 100%.

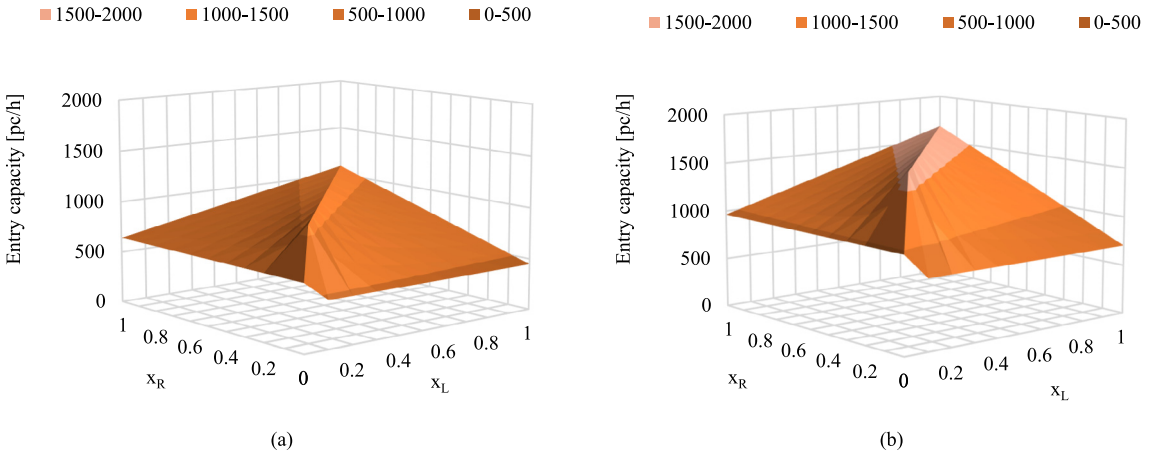

Fig. 8. Entry Capacity, Scenario 2. a) MPL = 0%; b) MPL = 100%.

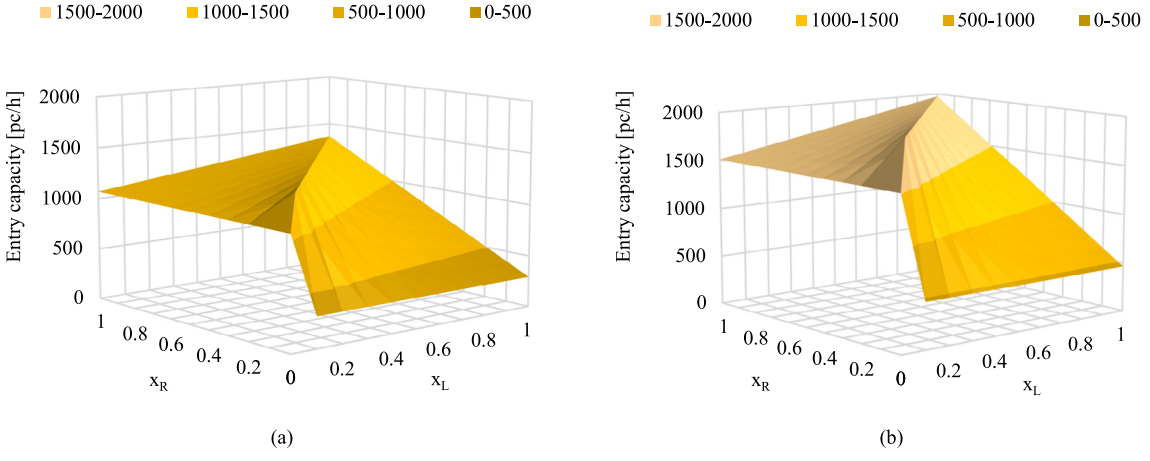

Fig. 9. Entry Capacity, Scenario 3. a) MPL = 0%; b) MPL = 100%.

Table 3
Scenarios considered for the capacity estimation of arms 1.

Scenario	Description	MPLs
Scenario 1	$v_{c,1e}$ = 500 pc/h, $v_{c,1i}$ = 500 pc/h, v_i^{ped} = 0 p/h, $\alpha = \beta = \gamma = \delta$ = 0.8, $R_1 = R_4$ = 12 m	MPL1 = 0%, MPL2 = 100%
Scenario 2	$v_{c,1e}$ = 750 pc/h, $v_{c,1i}$ = 250 pc/h, v_i^{ped} = 0 p/h, $\alpha = \beta = \gamma = \delta$ = 0.8, $R_1 = R_4$ = 12 m	MPL1 = 0%, MPL2 = 100%
Scenario 3	$v_{c,1e}$ = 250 pc/h, $v_{c,1i}$ = 750 pc/h, v_i^{ped} = 0 p/h, $\alpha = \beta = \gamma = \delta$ = 0.8, $R_1 = R_4$ = 12 m	MPL1 = 0%, MPL2 = 100%

Table 4
Level of service in function of the mean delay.

LEVEL OF SERVICE	Mean delay (volume/capacity < 1)	Volume-to-Capacity Ratio (volume/capacity > 1)
A	0 ÷ 10 (s/pc)	F
B	10 ÷ 15 (s/pc)	F
C	15 ÷ 25 (s/pc)	F
D	25 ÷ 35 (s/pc)	F
E	35 ÷ 50 (s/pc)	F
F	> 50 (s/pc)	F

where $D_{j,R}{}^{ped}$, $v_{j,R}$, $D_{j,L}{}^{ped}$ and $v_{j,L}$ are respectively delays and flow rates at the two lanes of the entry j. Similarly, the queue for each entry lane and the mean queue at the generic entry j can be estimated with the following relationships:

$$Q_{J,R}^{ped} = 900 \cdot T \cdot \left[\frac{v_{eJ,R}}{C_{J,R}^{ped}} - 1 + \sqrt{\left(\frac{v_{eJ,R}}{C_{J,R}^{ped}} - 1 \right)^2 + \frac{\left(\frac{3600}{C_{J,R}^{ped}} \right) \cdot \left(\frac{v_{eJ,R}}{C_{J,R}^{ped}} \right)}{150 \cdot T}} \right] \cdot \frac{C_{J,R}^{ped}}{3600} \quad (55)$$

$$Q_{J,L}^{ped} = 900 \cdot T \cdot \left[\frac{v_{eJ,L}}{C_{J,L}^{ped}} - 1 + \sqrt{\left(\frac{v_{eJ,L}}{C_{J,L}^{ped}} - 1 \right)^2 + \frac{\left(\frac{3600}{C_{J,L}^{ped}} \right) \cdot \left(\frac{v_{eJ,L}}{C_{J,L}^{ped}} \right)}{150 \cdot T}} \right] \cdot \frac{C_{J,R}^{ped}}{3600} \quad (56)$$

$$Q_j = \frac{Q_{J,R}^{ped} \cdot v_{J,R} + Q_{J,L}^{ped} \cdot v_{J,L}}{v_{eJ,R} + v_{eJ,L}} \quad (57)$$

Fig. 10 and Fig. 11 show the mean entry delay and mean entry queue variation at entry 1 in function of the degree of saturation of each lane (no pedestrian flow) for Scenario 1: $v_{c,1e} = v_{c,1i} = 500$ pc/h, $\alpha = \beta = \gamma = \delta = 0.8$, R1 = R4 = 12 m. Once again, CAVs may produce remarkable effects on the turbo roundabouts performance with a significant reduction of delays and queues in case of the MPL = 100% (Fig. 10b) with respect to traffic conditions in which traffic streams are composed by only traditional vehicles (MPL = 0%, cf. Fig. 10a). For reasons of synthesis, the results of Scenarios 2 and 3 (cf. Table 3) are not reported here, which in any case give rise to delay and queue variations similar to those of Figs. 10 and 11.

Figs. 12 and 13 exemplifies the variation of mean delays and queues for arm 1 (Fig. 2) as a function of the entry total flow and for different MPLs of CAVs, under given traffic boundary conditions. In particular, Fig. 12a depicts the delay curves for a case of balanced flows in the outer and inner circulating lanes ($v_{c,1e} = v_{c,1i} = 500$ pc/h), instead Fig. 12b illustrates the outcomes for a case of unbalanced circulating flows ($v_{c,1e} = 750$ pc/h, $v_{c,1e} = 250$ pc/h). In both of the analysed scenarios, the entry mean deals increase with the increase of entry flows; in addition, the increase in MPLs of CAVs produces significant benefits in terms of delays and queue reductions.

Even if the proposed theoretical model is "general", it is clear that the measure of effectiveness (capacities, delays and queues) depend on $t_{c,CAVs}$ and $t_{f,CAVs}$ values. Future experimental data, obtained from real-world analyses, will allow calibrating the model, once more realistic values of $t_{c,CAVs}$ and $t_{f,CAVs}$ will be available. However, it is possible to infer that reductions in $t_{c,CAVs}$ and $t_{f,CAVs}$ values with respect to those estimated in this article will determine capacity increases and reductions in delays and queues.

3. CAVs coordination to maximize the total capacity

One of the main objectives of vehicle communication technologies is to increase traffic operations through an exchange of data among vehicles and infrastructure. CAVs can increase the intersection capacity by adopting several strategies including distributing flows among shared lanes. Several procedures for improving traffic operations at intersections to take advantage of the CAVs in traffic streams have been suggested recently. These procedures can be classified into reservation and trajectory-based optimization schemes (Martin-Gasulla and Elefteriadou, 2019). This article hypothesizes a turbo roundabout manager that offers optimal trajectories to incoming vehicles to maximize the total capacity and therefore minimize control delay. The proposed procedure is graphically described in Fig. 14. In this Figure, the control area specifies where CAVs

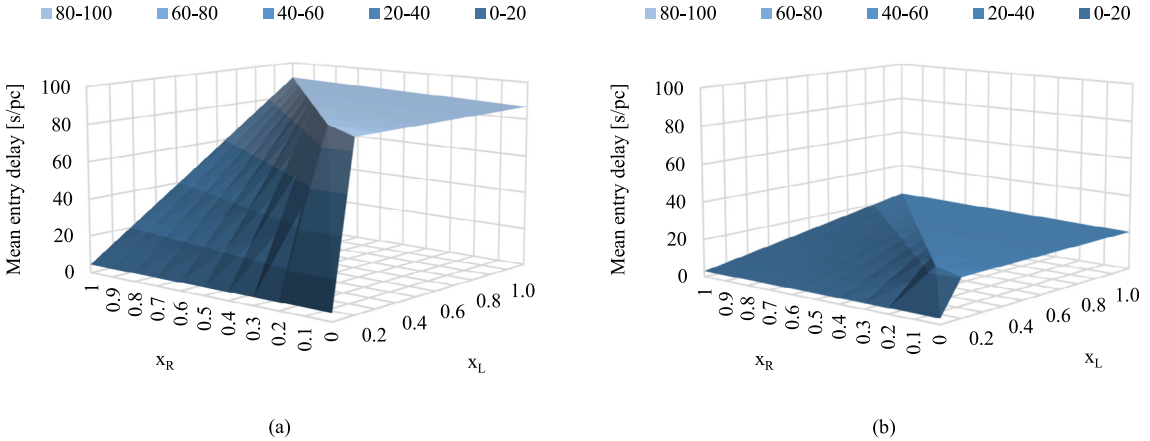

Fig. 10. A) mean entry delay, Scenario 1. a) MPL = 0%; b) MPL = 100%.

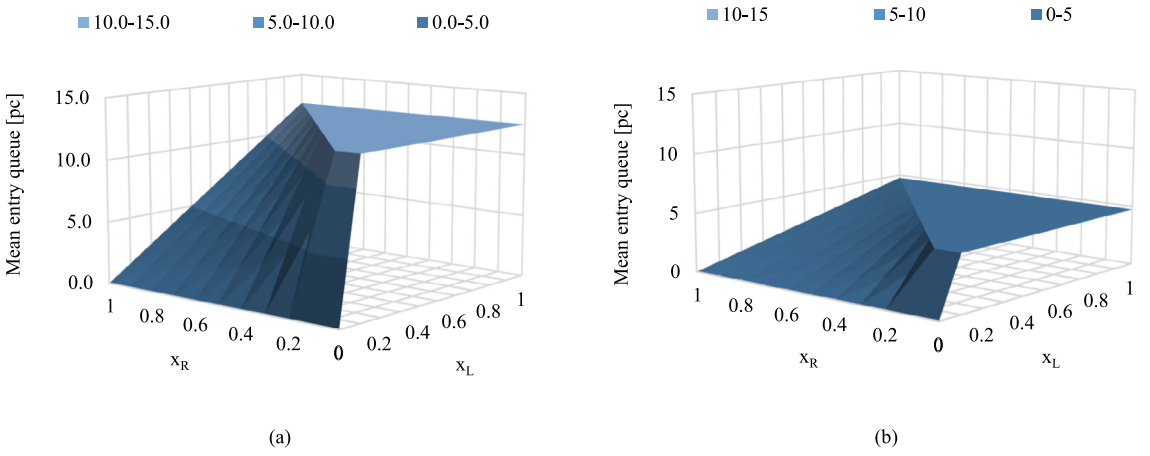

Fig. 11. A) Mean entry queue, Scenario 1. a) MPL = 0%; b) MPL = 100%.

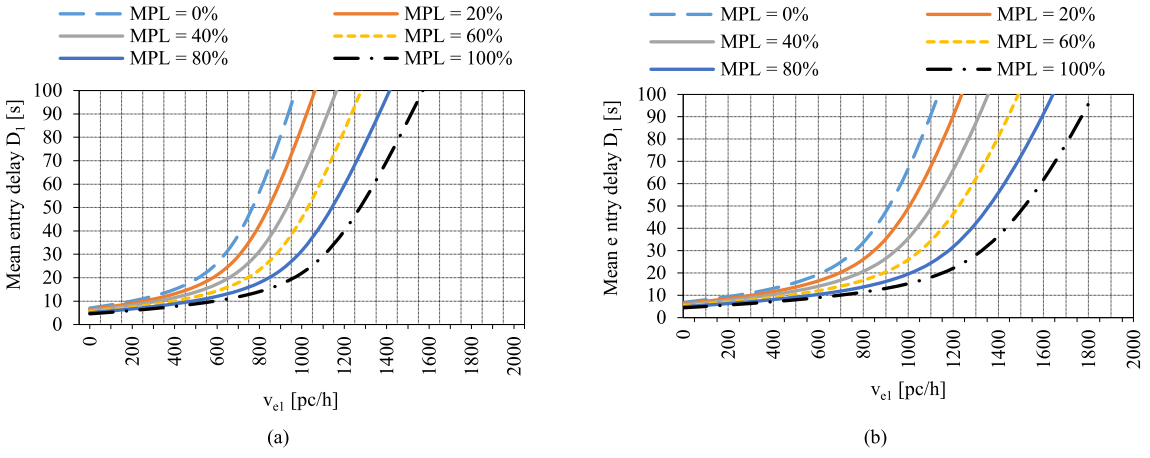

Fig. 12. Mean entry delay in function of conflicting flow rate and MPLs. $v_{1,R} = v_{1,L} = 0.5 \cdot v_1$, $\alpha = \beta = \gamma = \delta = 0.8$. a) $v_{c,1e} = v_{c,1i} = 500$ pc/h; b) $v_{c,1i} = 250$ pc/h $v_{c,1e} = 750$ pc/h.

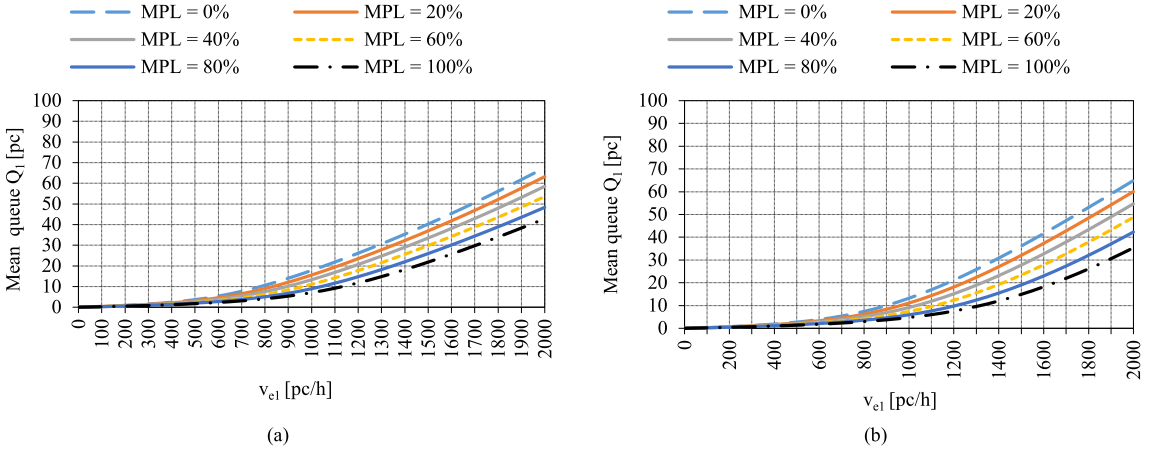

Fig. 13. Mean queue in function of conflicting flow rate and MPLs. $v_{1,R} = v_{1,L} = 0.5 \cdot v_1$, $\alpha = \beta = \gamma = \delta = 0.8$. a) $v_{c,1e} = v_{c,1i} = 500$ pc/h; b) $v_{c,1i} = 250$ pc/h $v_{c,1e} = 750$ pc/h.

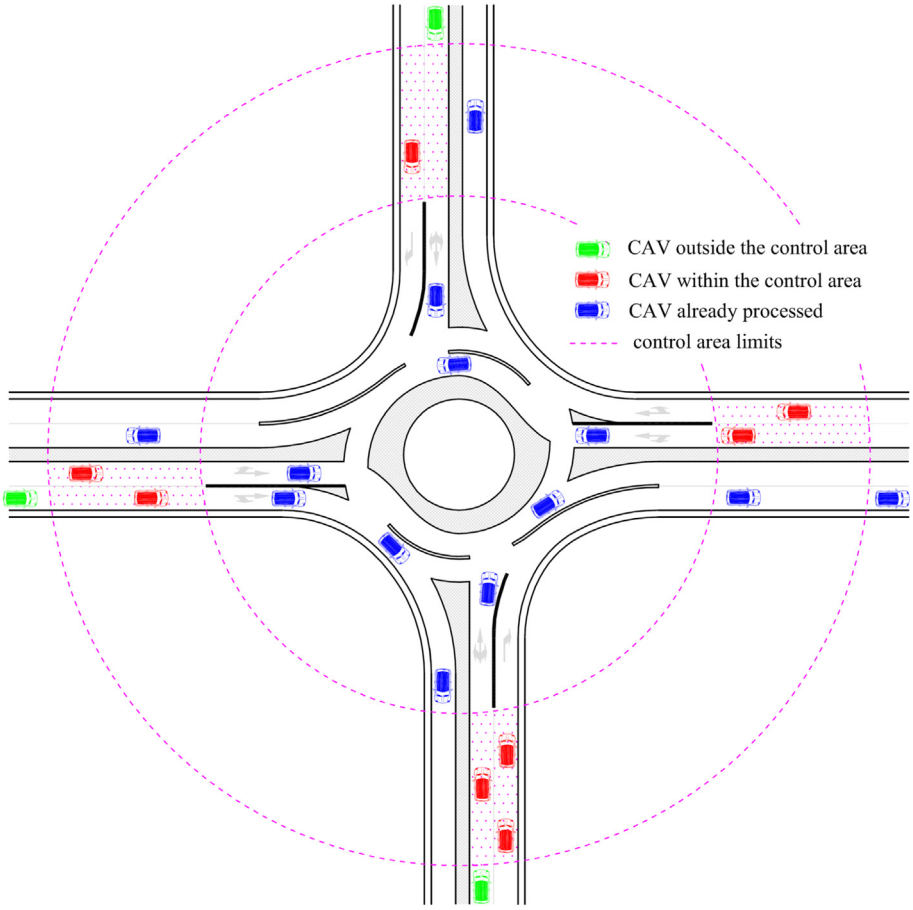

Fig. 14. Turbo roundabouts Manager scheme.

start to communicate with the turbo roundabout manager; in particular, the communication range is depicted by the magenta circumferences. Within this area, here called the management area (MA), CAVs can provide some kinematic information such as instantaneous position, speed, and acceleration, to the turbo roundabout manager and receive optimized trajectories to maximize the total capacity of the intersection. In particular, the Turbo Roundabout Manager should distribute and channel the flows of CAVs between the right and left lanes of each entry to maximize the capacity of the turbo roundabout. For every traffic distribution, the distribution factors α, β, γ, δ (cf. Eqs. (1)–(24)) change and therefore the total capacity of the turbo roundabout varies.

Once CAVs leave the MA through their desired exit arm, they are out of the coordination system. Therefore, the main problem of the coordination system is to find the values of the maneuver distribution factors α, β, γ, δ that maximize the turbo roundabout capacity for given traffic demand and distribute the traffic flow accordingly. Consequently, the first problem to be solved is the estimation of the total capacity of the turbo roundabout which is the turbo roundabout's ability to serve traffic when each arm is in saturation conditions. To this end, the following procedure can be adopted under the hypothesis of steady-state traffic conditions. In a given interval of time ΔT, the entry traffic demand of the turbo roundabout can be expressed by the vector:

$$v_e = [v_{ej}] \quad j = 1, 2, \cdots, 4 \tag{58}$$

for a traffic distribution matrix

$$P_{O/D} = [P_{j,k}] \quad j, k = 1, 2, \cdots, 4 \tag{59}$$

the origin/destination matrix of traffic demand $M_{O/D}$ is calculated as follows:

$$M_{O/D} = P_{O/D} \cdot v_e = [v_{jk}] \quad j, k = 1, 2, \cdots, 4 \tag{60}$$

In the present research, the total capacity (TC) is obtained as the sum of the entry flows $v_{e,j}$ under the condition that the degree of saturation of at least one of the two entry lanes of each arm is equal to 1:

$$\begin{cases} TC = \sum_{j=1}^{4} v_{ej} \\ \max\left(\frac{v_{ej,R}}{C_{j,R}^{ped}}; \frac{v_{ej,L}}{C_{j,L}^{ped}}\right) = 1 \quad \forall j \end{cases} \tag{61}$$

In Eq. (61) the entry flows $v_{e,j}$ are calculated by solving a system of equations in the j = 4 unknowns $v_{e,j}$. To determine total capacity TC a proper iterative method should be implemented, as explained in (Mauro, 2010). It is worth underlining that total capacity is a function only of the traffic percentage matrix $P_{O/D}$, and, therefore, it can be determined starting with an arbitrary traffic demand vector $v_e = [v_{ej}]$. The histogram in Fig. 15 provides a visualization of the total capacity values for various MPLs of CAVs and three traffic distribution matrices: $P_{O/D}$ 1 = 100% of entering vehicles turn right, $P_{O/D}$ 2: 100% of entering vehicles cross the roundabout, $P_{O/D}$ 3 = 100% of entering vehicles turn left. For every value of MPL the maximum TC is reached in the case in which all the vehicles turn right. Fig. 16 demonstrates that for the matrix $P_{O/D}$ 2 the total capacity values can variate significantly in function of the distribution factors of the maneuvers between the right lane and the left lane of each entry. For every MPL of CAVs the maximum TC is reached for $\alpha = \beta = \gamma = \delta = 50\%$.

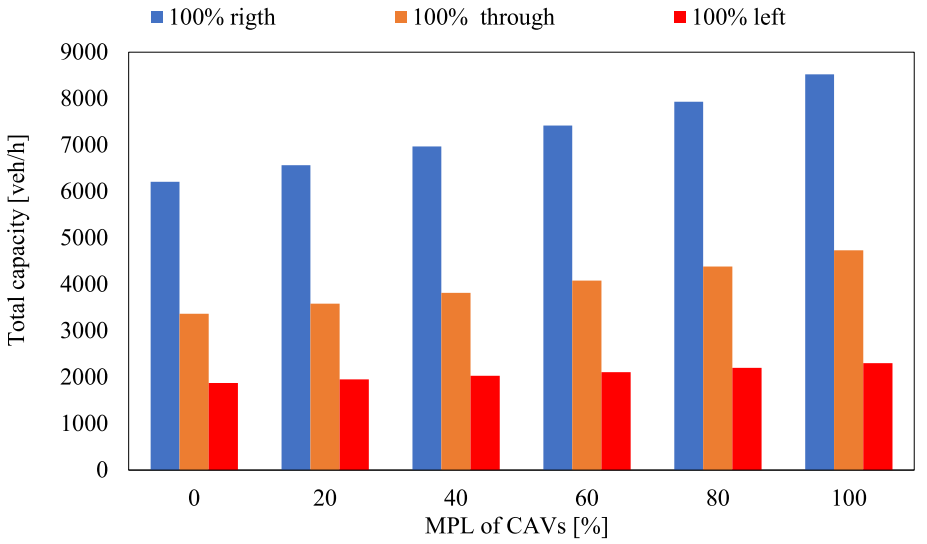

Fig. 15. Total capacity for different MPLs of CAVs and traffic distribution matrices.

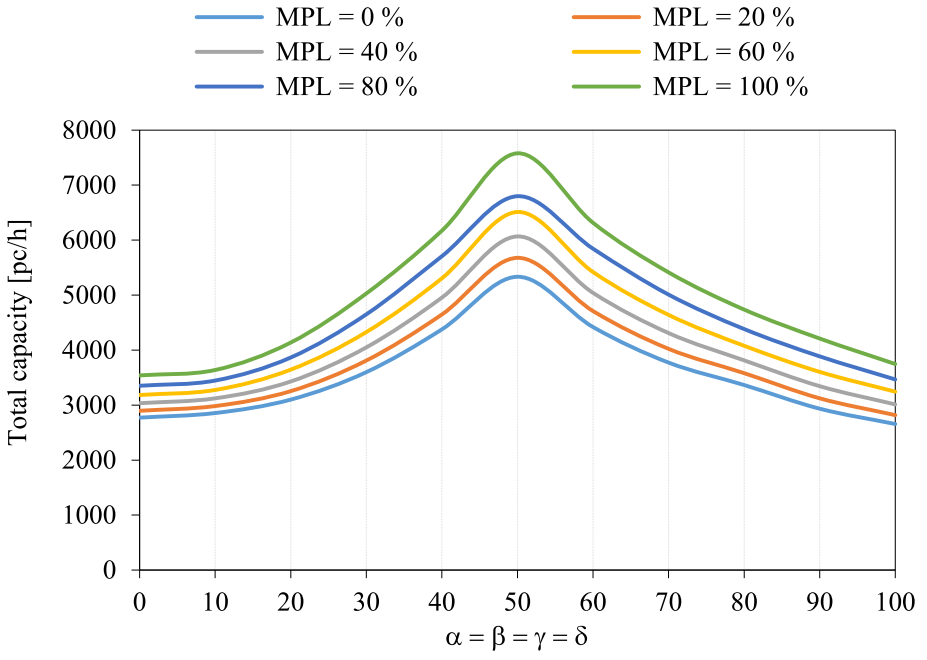

Fig. 16. Total capacity variation in function of different MPL_S of CAVs ($P_{O/D}$ 2).

For instance, considering the MPL = 100%, the TC (7579 pc/h) is 42% higher than the TC value (5334 pc/h) calculated for MPL = 0%.

Moreover, for every MPL, the TC decreases when α, β, γ and δ are close to 0% and 100%. Very similar results can be obtained by modifying the traffic distribution matrices. It can be deduced that a control system able to adapt trajectories of incoming vehicles outperforms the expected operation of traditional vehicles. Therefore, even better performance in terms of total capacity may be realised when vehicles obtain their trajectories in advance instead of providing the right-of-way in front of the Yield line. Hence, for the MPL = 100%, the turbo roundabout manager should distribute and channel the entering flows by respecting a specific condition between the distribution factors α, β, γ and δ, maximizing the total capacity.

4. Conclusions

The advanced development of wireless communication technologies and automation systems will allow the implementation of a new generation of vehicles soon, namely connected and automated vehicles (CAVs), on the urban and extra-urban road network. Due to the potential capability to communicate with each other and with road infrastructures, CAVs can negotiate the right-of-way at turbo roundabouts and coordinate their trajectories without the indications of road signals. Based on CAVs technologies, an Autonomous Intersection Manager system (AIMS) can be customized to improve the capacity of turbo roundabouts.

The article sets out to present a closed-form model to estimate the entry capacity (EC) and the total capacity (TC) of basic turbo roundabouts in CAVs environments, taking into consideration several market penetration levels of automated vehicles and the corresponding values of the critical gap $t_{c,m}$ and $t_{f,m}$ associated to mixed traffic of human-driven vehicles (HDVs) and CAVs. Using a lane-by-lane approach and formulations based on the gap acceptance theory, it has been shown that the entry capacity of turbo roundabouts depends not only on entry lane capacities but also on the flows along inner and outer circulating lanes, users' behavior (psycho-technical parameters of HDVs and CAVs), geometry (in terms of circulating lanes radii) and distribution factors (α, β, γ, δ) of maneuvers between the right lane and the left lanes of each arm and market penetration levels (MPLs) of CAVs.

Different traffic scenarios were analysed. The results demonstrate that with the increase in the MPLs of CAVs, the entry capacity increases (up to 57%) and consequently delays and queues decrease. It is worth underlining that the incoming traffic demand under the CAVs environment can also modify the turbo roundabout total capacity (TC). Moreover, CAVs could be able to increase the capacity of intersections by adopting different strategies, including an adequate distribution of flows between shared lanes. The research demonstrates that the total capacity may vary significantly in function of the maneuver distribution factors (α, β, γ, δ) between the right and the left lanes of each entry. In particular, for the traffic distribution $P_{O/D}$ 2 (100% of entering vehicles cross the turbo roundabout) the maximum TC is reached for $\alpha = \beta = \gamma = \delta = 50\%$. As a matter of fact, for a fleet of 100% CAVs the TC is 42% higher than the TC value obtained for a fleet of 100% HDVs. Similar benefits can be obtained by varying traffic distribution matrices. In general, the outcomes revealed that CAVs can improve the MOE of turbo roundabouts. However, as CAVs technology is a relatively new field of research, this article has a few limitations. In particular, the critical gap $t_{c,CAVs}$ and the follow-up time $t_{f,CAVs}$ assumed for CAVs may not represent real-life values, this is because currently there is a lack of empirical data that would make them reliable. Nevertheless, based on the current scientific literature, it can be argued that the main results of this research, in terms of capacities, delays and queues, can be considered reasonable estimates.

Future work could involve analyzing a wider range of traffic scenarios, analysis methods (analytical procedures and microscopic simulations) and turbo roundabout layouts and examining the comparison of different innovative roundabout layouts in urban areas where the presence of vulnerable road users cannot be neglected.

Funding details

This study received no funding from any source.

Disclosure Statement

There is no any known financial interest or benefit to disclose.

Declaration of Competing Interest

The authors declare that they have no known competing financial interests or personal relationships that could have appeared to influence the work reported in this paper.

References

AASHTO, 2011. A Policy on Geometric Design of Highways and Streets, 6th Edition, (commonly referred to as the "Green Book").
Akcelik, R., 1994. Gap-acceptance modelling by traffic signal analogy. Traffic Engineering±. Control 35 (9), 498–501.

Akcelik, R., 1997. Lane-by-lane modelling of unequal lane use and flares at roundabouts and signalised intersections: the SIDRA Solution. Traffic Engrg. Control, London 38 (7/8).
Anagnostopoulos, A., Kehagia, F., 2020. CAVs and roundabouts: Research on traffic impacts and design elements. Transp. Res. Procedia 49, 83–94.
Brilon W., Stuwe B., Drews O., 1993Sicherheit und Leistungsfähigkeit von Kreisverkehrsplätzen. Institute for Traffic Engineering, Ruhr Universität, Bochum (Deutschland).
Brilon, W., Bondzio L., Wu, M., 1997. Unsignalized Intersection in Germany. A State of the Art. In: 2nd International Symposium for unsignalized intersection, Portland/Oregon (USA).
Brilon, W., Bondzio, L., Weiser, F., 2014. Experiences with turbo- roundabouts in Germany. In: 5th Proc., Rural Roads Design Meeting, Copenhagen. Bochum.
Corriere, F., Guerrieri, M., Ticali, D., Messineo, A., 2013. Estimation of air pollutant emissions in flower roundabouts and in conventional roundabouts. Arch. Civ. Eng. 59 (2), 229–246. https://doi.org/10.2478/ace-2013-0012.
Easa, S.M., You, Q.C., 2023. Intersection Sight Distance Requirements for Basic Turbo Roundabouts. J. Transport. Eng. Part A: Syst. 149 (21).
Fortuijn, L.G.H., 2009. Turbo roundabouts: Estimation of capacity. Transp. Res. Rec. 2130 (1), 83–92. https://doi.org/10.3141/2130-11.
Gill, V., Kirk, B., Godsmark, P., Flemming, B., 2015. Automated Vehicles: The Coming of the Next Disruptive Technology. Ottawa: The Conference Board of Canada. Ottawa, Ontario Canada.
Guerrieri, M., 2021. Smart roads geometric design criteria and capacity estimation based on AV and CAV emerging technologies. A case study in the trans-European transport network. Int. J. Intell. Transp. Syst. Res. 19 (2), 429–440.
Guerrieri, M., Corriere, F., Lo Casto, B., Rizzo, G., 2015. A model for evaluating the environmental and functional benefits of innovative roundabouts. Transp. Res. Part D: Transp. Environ. 39, 1–16.
Guerrieri, M., Mauro, R., Parla, G., Tollazzi, T., 2018. Analysis of kinematic parameters and driver behavior at turbo roundabouts. J. Transport. Eng. Part A: Syst. 144, (6) 04018020.
HCM 7th Edition, 2022. (Highway Capacity Manual, 7th Edition): A Guide for Multimodal Mobility Analysis. TRB.
Jiang, Q., Schroeder, B., Ma, J., Rodegerdts, L., Cesme, B., Bibeka, A., Morgan, A., 2022. Developing highway capacity manual capacity adjustment factors for connected and automated traffic on roundabouts. J. Transport. Eng. Part A: Syst. 148 (5).
Martin-Gasulla, M., Elefteriadou, L., 2019. Single-lane roundabout manager under fully automated vehicle environment. Transport. Res. Rec. 2673 (8), 439–449.
Martin-Gasulla, M., Sukennik, P., Lohmiller, J., 2019. Investigation of the impact on throughput of connected autonomous vehicles with headway based on the leading vehicle type. Transp. Res. Rec. 2673 (5).
Mauro, R., 2010. Calculation of Roundabouts: Capacity, Waiting Phenomena and Reliability. Springer-Verlag, Berlin Heidelberg, p. 2010.
Mauro, R., Guerrieri, M., 2016. Comparative life-cycle assessment of conventional (double lane) and non-conventional (turbo and flower) roundabout intersections. Transp. Res. Part D: Transp. Environ. 48, 96–111. https://doi.org/10.1016/j.trd.2016.08.011.
Mohebifard, R., Hajbabaie, A., 2021. Connected automated vehicle control in single lane roundabouts. Transport Res. Part C: Emerg. Technol. 131, 12.
Rodegerdts, L., Blogg, M., Wemple, E., Myers, E., Kyte, M., Dixon, M., List, G., Flannery, A., Troutbeck, R., Brilon, W., 2007. Appendixes to NCHRP Report 572: Roundabouts in the United States. NCHRP Web-Only Document, p. 94.
Song, Y., Hu, X., Lu, J., Zhou, X., 2022. Analytical approximation and calibration of roundabout capacity: A merging state transition-based modeling approach. Transp. Res. B Methodol. 163, 232–257.
Tollazzi, T., 2014. Alternative Types of Roundabouts: An Informational Guide. Springer.
Tollazzi, T., Rencelj, M., Turnsek, S., 2011. Slovenian experiences with alternative types of roundabouts: 'Turbo' and 'flower' roundabouts. Proc., 8th Int. Conf. on Environmental Engineering, ICEE 2011, 1220–1226. Vilnius, Lithuania: Vilnius Gediminas Technical Univ.
Troutbeck, R., 1989. Evaluating the Performance of a Roundabout. Australian Road Research Board, Vermont South.
Tumminello, M.L., Macioszek, E., Granà, A., Giuffrè, T., 2022. Simulation-based analysis of "What-If" scenarios with connected and automated vehicles navigating roundabouts. Sensors 22, 6670. https://doi.org/10.3390/s22176670.
Vasconcelos, A.L.P., Silva, A.B., Seco, Á.J.M., 2014. Capacity of normal and turbo-roundabouts: Comparative analysis. Proc. Inst. Civ. Eng. Transp. 167 (2), 88–99.
Wu, N., 2001. A universal procedure for capacity determination at unsignalized (priority-controlled) intersections. Transp. Res. Part B Methodol. 35 (6), 593–623.
Wu, Y., Zhu, F., 2021. Junction management for connected and automated vehicles: Intersection or roundabout? Sustainability (Switzerland) 13 (16).
Yap, Y.H., Gibson, H.M., Waterson, B.J., 2013. An international review of roundabout capacity modelling. Transp. Rev. 33 (5), 593–616.
Zhao, L., Malikopoulos, A., Rios-Torres, J., 2018. Optimal control of connected and automated vehicles at roundabouts: An investigation in a mixed-traffic environment. IFAC-PapersOnLine 51 (9), 73–78. https://doi.org/10.1016/j.ifacol.2018.07.013.
Zmud, J., Williams, T., Outwater, M., Bradley, M., Kalra, N., Row, D., 2018. NCHRP Research Report 896 - Updating Regional Transportation Planning and Modeling Tools to Address Impacts of Connected and Automated Vehicles, Volume 2: Guidance. The National Academies Press, Washington, DC.